Modeling of Subcritical Penetration into Sediments Due to Interface Roughness

Eric I. Thorsos, Darrell R. Jackson, John E. Moe,[1] and Kevin L. Williams

Applied Physics Laboratory, University of Washington
1013 NE 40th Street
Seattle, Washington 98105
E-mail: eit@apl.washington.edu, drj@apl.washington.edu, jemoe@aol.com, williams@apl.washington.edu

Abstract

Recent experimental results reveal acoustic penetration into sandy sediments at grazing angles below the critical angle. We have been investigating a mechanism for subcritical penetration based on scattering at a rough water–sediment interface. Using perturbation theory, a numerically tractable three-dimensional model has been developed for simulating experiments. Data–model comparisons show that interface roughness is a viable hypothesis for the observed subcritical penetration.

1. Introduction

High-frequency acoustic penetration into seafloor sediment at low grazing angles is of interest for buried mine detection. For sandy sediments the critical angle can be in the 25° to 30° range, which suggests that penetration at lower grazing angles might be quite limited. However, recent experimental results reported by Chotiros [1] reveal acoustic penetration into sandy sediments at grazing angles below the critical angle over a broad frequency range (5–80 kHz). In addition, the propagation speed in the sediment was inferred to be near 1200 m/s, significantly lower than the compressional sound speed of about 1700 m/s in unconsolidated 28. March 1997sands. Chotiros interprets these results to indicate the excitation of a Biot slow wave in the sediment. Subcritical acoustic penetration into sediments has also been reported by Lopes [2].

We have investigated an additional mechanism for subcritical penetration based on scattering at a rough water–sediment interface. Examples of data–model comparisons will be given that show interface roughness is a viable hypothesis for the observed subcritical penetration. For this mechanism, the propagation speed of the sound penetrating the sediment is the standard compressional wave speed of about 1700 m/s, but the apparent speed found through a processing technique similar to that used in the experiments can be significantly less and ranges from about 1200 m/s to about 1500 m/s depending on the roughness conditions assumed. A simple explanation for this lower apparent speed will be given. We believe that further field experiments are necessary to clarify whether the observed subcritical penetration is due to the Biot slow wave mechanism, to the interface roughness mechanism, or to possibly some other mechanism.

Before considering simulations of experiments, we present results in Section 2 for the penetrating field in two dimensions obtained with an exact integral equation method. These results show the potential for a rough interface to couple sound into the sediment at subcritical grazing angles. In order to simulate experiments a tractable three-dimensional (3-D) model is required that accounts for the finite pulse lengths used, and such a model has been developed using perturbation theory. In Section 3 exact results are used to demonstrate that perturbation theory is valid in a 2-D geometry for roughness conditions of interest and thus should be valid for the 3-D geometry as well. In Section 4 perturbation theory is used in a 3-D model for data–model comparisons of apparent sound speed, propagation direction, and attenuation in the sediment. A concluding discussion is given in Section 5.

[1]Presently at Acuson, 1220 Charleston Rd., P.O. Box 7393, Mountain View, CA 94039.

2. Exact simulations of acoustic penetration into sediment

In our work to date, we have modeled the sediment as a fluid supporting only compressional waves, since for sand sediments it can be shown that coupling into shear waves is negligible. The problem of scattering from and transmission through a rough two-fluid interface can be solved exactly in the cw case for particular rough interface realizations using an integral equation method. Because of high computational requirements, this method is essentially limited to a 2-D geometry with a 1-D rough interface. Nevertheless, such results illustrate that surface roughness can couple acoustic energy into sediments when the incident grazing angle is below the critical angle. Space does not permit a detailed exposition of the integral equation method here. A formulation for electromagnetic scattering at a rough surface separating two media (closely analogous to the two-fluid case) is given in [3], and the simpler case of a single fluid with rough surface subject to a Dirichlet boundary condition is treated in [4].

With a specified incident pressure field on the rough surface, solution of the integral equation (actually two coupled integral equations) gives the field and the normal derivative of the field on the surface. With these quantities known, it is possible to compute, via the Helmholtz-Kirchhoff integral formula, the field at any point on either side of the interface and thus construct maps of the field structure. Absorption in the sediment is incorporated by using a complex wavenumber in the fluid below the interface.

To illustrate the effects of roughness on acoustic penetration into sediment, we consider parameters similar to those for the Acoustic Testbed Experiment (ATBE) near Panama City [1] to be discussed further in Section 4. Denoting the sound speed and density by c_1 and ρ_1 in the water and c_2 and ρ_2 in the sediment, respectively, we use $c_2/c_1 = 1.13$ (which gives a critical angle of 27.8°), $\rho_2/\rho_1 = 2.0$, and a sediment absorption of 0.5 dB/m/kHz. The 2-D spectrum of sediment roughness was not measured during ATBE. For numerical simulations in two dimensions, we require a 1-D roughness spectrum $W(K)$, which we model in the following modified power-law form:

$$W(K) = w_1 / \left(K^2 + K_L^2\right); \tag{1}$$

$W(K)$ is defined such that $W(-K) = W(K)$, where K is the spatial wavenumber, and the mean square surface height, h^2, is obtained by integrating $W(K)$ over all K. In (1) a "lower cutoff," K_L, has been introduced to yield a finite mean square surface height. A similar cutoff will be used in Section 4 with the 2-D roughness spectrum and discussed further there. An upper cutoff, $K_U = 2k_1$, where k_1 is the acoustic wavenumber in the water, is also imposed on (1) such that $W(K) = 0$ if $|K| > K_U$. For the example in this section, $w_1 = 0.02$ cm and $K_L = 0.1$ cm^{-1}, which yield a roughness parameter $k_1 h = 0.66$ at a frequency of 20 kHz. The results shown are not changed qualitatively if K_L is made smaller or if K_U is made larger.

Examples of pressure fields obtained with the integral equation method for both a flat and a rough surface are shown in Fig. 1. In these figures the mean water–sediment interface is at 0.0 cm on the vertical scale, and the color display is linear in pressure. A 20-kHz plane wave of unit magnitude is incident from the left at a grazing angle of 20°, which is below the critical angle of 27.8°; this incident wave has been omitted to simplify the field structure. In Fig. 1(a) the surface is flat, and the phase fronts of the reflected wave can be seen moving up and to the right above the interface. For this flat surface case, the field in the sediment is evanescent; it decreases exponentially with depth and has a significant magnitude for only about a wavelength into the sediment. In Fig. 1(b) the rough surface realization is consistent with the spectrum given by (1). Energy can be seen to radiate down into the sediment at relatively steep angles, in part because absorption will tend to remove energy propagating closer to the horizontal.

One might expect acoustic penetration into the sediment to occur at regions along the surface where the local grazing angle (accounting for the local surface slope) exceeds the critical angle. However, acoustic penetration due to roughness occurs even if this condition is not met anywhere on the surface. It is evident from Fig. 1 that the field scattered down into the sediment is spatially incoherent, while for the Biot slow wave hypothesis, the penetrating field would be a spatially coherent wave (assuming that interface and volume scattering effects are negligible.)

In order to see if the rough surface scattering mechanism could explain the acoustic penetration results reported by Chotiros, it is necessary to model the full 3-D experiment geometry, which is not practical using the integral equation approach. Thus, we have employed perturbation theory to account for the effects of scattering. In doing this, we sometimes consider levels of surface roughness, as indicated by the parameter $k_1 h$, which are uncomfortably large for the normal application of lowest-order perturbation theory. Therefore, we first turn to the question of the applicability of perturbation theory for our regime of interest. This is done in two dimensions, where integral equations results can serve as ground truth.

3. Validity of perturbation theory for acoustic scattering into sediment

Formally, we require $k_1 h << 1$ for lowest-order perturbation theory to be accurate in predicting bistatic scattering back into the water from a rough bottom that can be modeled as a homogeneous fluid. Numerical studies using the integral equation method show that, as $k_1 h$ increases, the inaccuracy of perturbation theory first becomes noticeable at a $k_1 h$ of about 0.3–0.4. For scattering into the sediment, however, numerical results show that perturbation theory accuracy extends to much

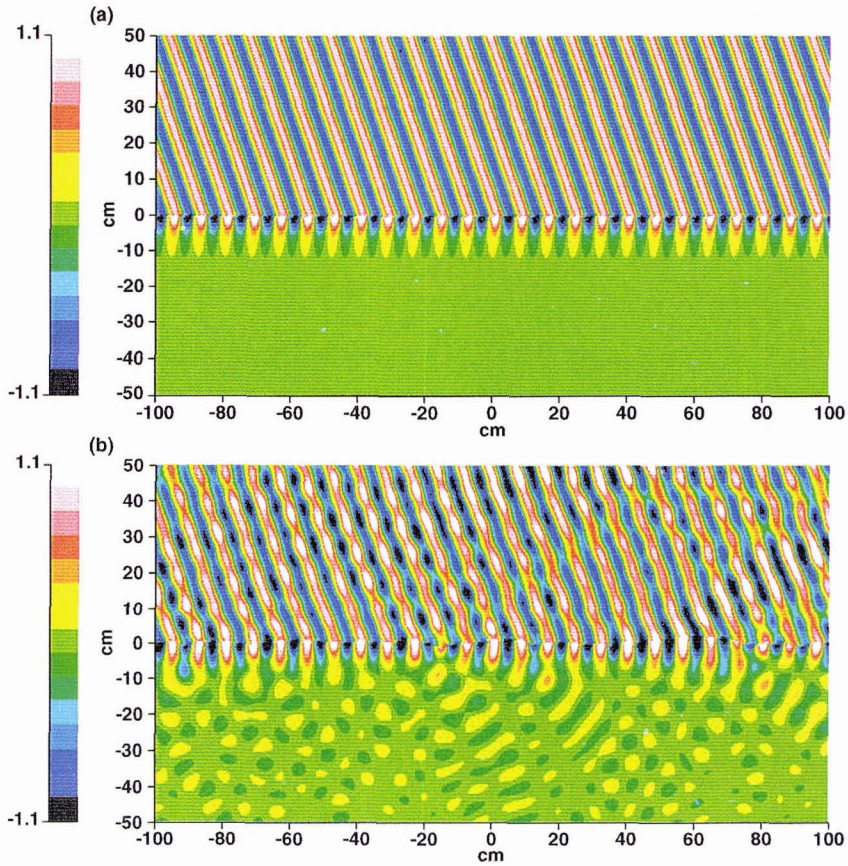

Figure 1. Pressure fields above (in water) and below (in sediment) a flat surface (a) and a rough surface (b) obtained for a 2-D geometry using the exact integral equation method. The incident field (not shown) is from the left at a grazing angle of 20°, which is below the critical angle of 27.8°.

higher roughness levels. Essentially, the smallness of the sound speed contrast between the water and sediment reduces the effective roughness of the interface for the transmission scattering problem. As a result, perturbation theory remains accurate for much larger $k_1 h$ than might be expected.

Here we simply illustrate this improved accuracy with an example without pursuing a fundamental explanation. Figure 2 shows a comparison between perturbation theory and exact integral equation bistatic scattering results for an example with $k_1 h = 1.0$. The sound speed and density ratios are the same as in Fig. 1, and the roughness spectrum is again given by (1) with $w_1 \approx 0.02$, but K_L has been reduced to 0.044 cm^{-1} to obtain $k_1 h = 1.0$. Again as in Fig. 1, the incident grazing angle of 20° is below the critical angle of 27.8°. For simplicity, absorption in the sediment has been suppressed in this example. For this two-dimensional scattering problem, the scattering strength is 10 $\log_{10}$ (σ), where σ is the bistatic scattering cross section given by $< I_s > r / I_i L$. Here I_i is the incident intensity on the surface of length L, and $< I_s >$ is the average intensity at far-field range r. With the integral equation method, the average scattered intensity was obtained using 50 surface realizations, and a tapered plane wave incident field was employed as described in [4]. Finally, for scatter back into the water, the coherent intensity (over the ensemble of surface realizations) was removed, leaving only the incoherent intensity, which is the appropriate quantity to compare with perturbation theory. For scatter into the sediment, there is no coherent field in the far zone since the incident angle is below the critical angle.

Figure 2 shows that for scattering back into the water lowest-order perturbation theory overpredicts the scattering level by about 1 dB near the specular direction (a scattering angle of 160°), which is not surprising since $k_1 h = 1.0$. Nevertheless, accuracy for scattering into the sediment is excellent, and this agreement extends to even higher values of $k_1 h$, well beyond

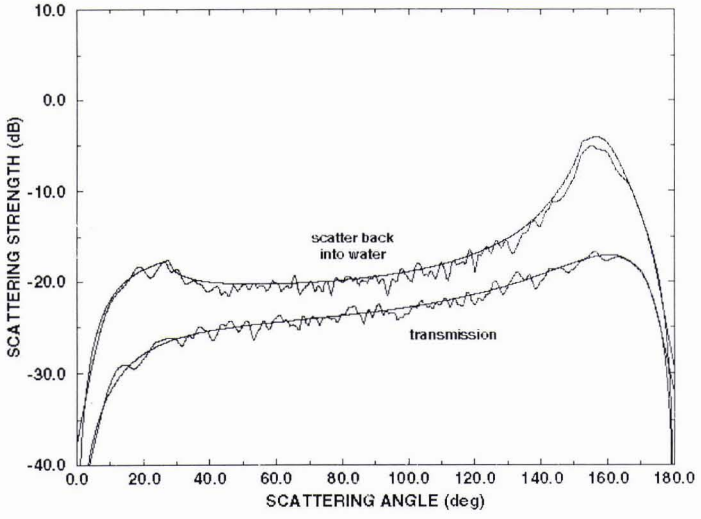

Figure 2. Bistatic scattering strengths for scattering from a rough sediment surface for a 2-D geometry. The smooth curves are obtained using lowest-order perturbation theory, and the fluctuating curves with the integral equation method. The incident grazing angle is 20°, the critical angle is 27.8°, and $k_1 h = 1.0$.

what is need for experiment simulations. In this comparison absorption in the sediment has been neglected. When absorption is included, the comparison is again excellent, except within about 10° of grazing where the situation becomes much more complicated. Low grazing angle paths will be unimportant in our experiment modeling, however, since these paths will be highly attenuated. Thus, we believe perturbation theory is highly accurate for simulating the effects of sediment roughness on acoustic penetration into sediment.

4. Simulation of measured acoustic penetration into sediment

In this section we use full 3-D simulations to examine whether the rough surface scattering mechanism for penetration into sediment can explain results reported by Chotiros [1]. In the experiment an acoustic projector on a movable tower transmitted short sound pulses to an array of buried hydrophones (Fig. 3). Because the projector was movable, the incident grazing angle could be varied, and (after processing) the temporal resolution was about 0.1 ms. The received signals from the buried array were used to deduce the propagation speed and direction in the sediment. Because the hydrophone locations were not known to the precision of a fraction of a wavelength, these deductions were made with an incoherent processing technique as described in [1]. When the incident grazing angle was well above the critical angle, the propagation speed deduced is consistent with the measured sediment sound speed of 1729 m/s, and the direction is consistent with Snell's law.

We consider 20-kHz ATBE results at an incident grazing angle of 12.7°, well below the critical angle of about 28°. Figure 4(a) (adapted from [1]) shows an ambiguity plot in sound speed and depression angle obtained from the experimental data indicating a propagation speed for this case of about 1300 m/s. For the region between the solid and dotted lines, the propagation direction and speed were considered consistent with Snell's law, given the experimental uncertainties [1].

A detailed description of the experiment simulation is given by Moe [5] and is only briefly summarized here. The intensity time series at each hydrophone is obtained as a sum of incoherent and coherent intensities, the latter being important only in the evanescent region near the interface. A Gaussian pulse with pressure envelope given by $\exp(-t^2/t_s^2)$ with t_s = 0.1 ms is used. The incoherent intensity is found by dividing the surface area into a large number of subareas and summing the time delayed contributions from each using the bistatic scattering cross section (lowest-order perturbation theory) appropriate for each subarea. The signal level is reduced by spherical spreading from the source to each area element and by spherical spreading and attenuation from each area element to each hydrophone. The coherent intensity is found ignoring interface roughness. This contribution can be expressed in terms of a Fourier transform of a quantity which itself is given by an integration over wave vector. Analytical approximations are often used for the latter integral based on a steepest descent solution [6], but here a full numerical evaluation is used.

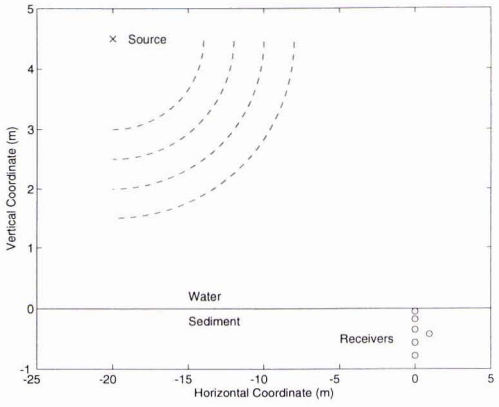

Figure 3. Simulation geometry for acoustic penetration measurements. Note exaggeration of vertical scale.

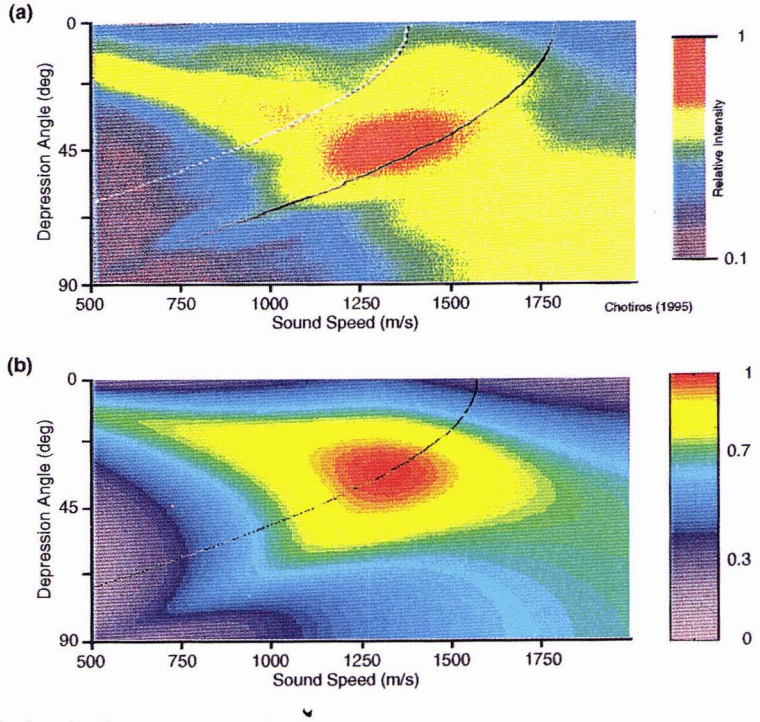

Figure 4. Ambiguity plot for apparent sound speed and propagation direction in sediment. (a) Experimental results reported by Chotiros [1] and (b) simulation results based on scattering from a rough sediment interface. The frequency is 20 kHz and the incident grazing angle is 12.7°. In (a) the region between the lines is considered consistent with Snell's law; in (b) points on the line are consistent with Snell's law.

A 2-D spectrum of surface roughness is needed to evaluate the perturbation theory cross section, and, as mentioned previously, the roughness spectrum was not measured during ATBE. Some guidance is provided by a spectrum obtained in the same region with similar water depths and sediment properties in 1984 [7], about 2 years before ATBE. These data can be represented in the isotropic form [8]

$$W(\mathbf{K}) = w_2 / K^3 \tag{2}$$

valid over a length scale range from about 50 cm down to 0.8 cm (for $2\pi/K$), where $w_2 = 6.2 \times 10^{-3}$ cm and $K = |\mathbf{K}|$. Unfortunately, owing to the spatial separation and the time lapse between the spectrum and penetration measurements, we cannot have confidence that (2) applies to the sediment surface near ATBE. In addition it is likely that the sediment was disturbed in the process of burying hydrophones. For simulations we have modified (2) with two different forms of low-wavenumber cutoffs: a "Gaussian" cutoff form

$$W(\mathbf{K}) = \frac{w_2}{K^3}\left[1 - \exp\left(-\frac{1}{2}K^2 a^2\right)\right]^2 \tag{3}$$

and an "algebraic" cutoff form

$$W(\mathbf{K}) = \frac{w_2}{\left(K^2 + K_L^2\right)^{3/2}}. \tag{4}$$

Using (3) with w_2 from (2) and with $a = 4$ cm yields a spectrum relatively rich in high-wavenumber structure. Doing the simulation with these parameters and using an incoherent processing technique similar to that used for the experimental data yields the ambiguity plot shown in Fig. 4(b), which agrees closely with Fig. 4(a). It must be emphasized that in this simulation the actual propagation speed in the sediment is 1729 m/s, but the apparent speed as measured by this processing method is close to 1300 m/s in this example. Snell's law is satisfied for points on the black line in Fig. 4(b), which passes through the maximum in the simulation ambiguity plot.

By using different choices for the form of the spectrum and for the low-wavenumber cutoff, we obtain apparent propagation speeds in roughly the 1200–1500 m/s range. As the low-wavenumber cutoff is reduced, the apparent speed increases and finally stabilizes at about 1500 m/s, becoming insensitive to further reductions. For example, using (4) with $K_L < 0.2$ cm^{-1} gives about 1500 m/s. Thus, if the spectrum were of the form of (2) down to length scales of about 30 cm or beyond, we would predict an apparent speed of about 1500 m/s. (The example in Fig. 1 should be consistent with this case.) With roughness spectra relatively richer in high-wavenumber components, apparent speeds in the 1100–1300 m/s range can be obtained.

In addition to propagation speed and direction in the sediment, attenuation in the sediment is also of interest. For ATBE Chotiros reports slow-wave attenuations of 30–40 dB/m at 20 kHz [1]. A fit to the signal levels for all six hydrophones used in the simulation of Fig. 4b yields an attenuation of 19 dB/m. However, if only the top three hydrophones are used in the fit, an attenuation of 36 dB/m is obtained. This difference occurs because the top hydrophone is strongly affected by the evanescent wave and by scattered waves propagating close to horizontally, whereas the signal at the deeper hydrophones is made up of scattered waves propagating more steeply.

5. Discussion

The way in which scattered waves traveling at the normal sediment compressional speed (c_2) can appear to be traveling at a much slower speed is illustrated in Fig. 5. Consider a short-pulse plane wave whose leading edge at some time is aligned with the arrows on the water side of the interface. Assume the pulse scatters at the surface and for simplicity propagates

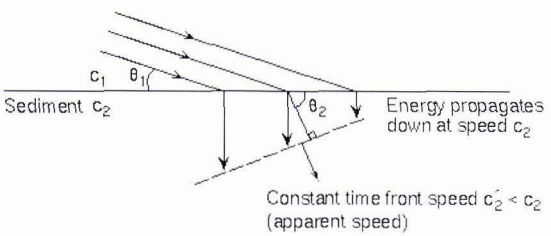

Figure 5. Schematic showing how scattering at the sediment interface can mimic a slow wave in the sediment. For simplicity energy is assumed to scatter straight down.

straight down. The leading edge will propagate down at speed c_2 and at some later time be aligned with the arrows shown in the sediment. If one assumes the propagation direction is normal to this leading edge (as done for these experiments and

in our simulations), the apparent speed will be $c_2' < c_2$. For c_2 of about 1700 m/s, for low-incident grazing angles, and for vertical propagation in the sediment, it is easy to show that c_2' is about 1100 m/s. As the mean propagation direction moves forward from vertical, c_2' increases so that a range of apparent speeds can be obtained depending on the mean propagation direction, which in turn depends on the properties of the sediment roughness spectrum. It is also easy to show that the apparent speed and direction will always be consistent with Snell's law in this simple model of a single propagation direction in the sediment, whether vertical or not.

In summary, we have shown that scattering from a rough water–sediment interface is a viable hypothesis for subcritical penetration into sediments. With a suitable choice of roughness spectrum, this mechanism can explain the observation of apparent slow wave speeds in sediments. Simulated attenuations are less than reported experimentally, but if the analysis is restricted to a subset of hydrophones closest to the surface, simulation results are consistent with the reported values. Acoustic penetration experiments with the roughness spectrum measured in the precise experimental area should be able to determine if scattering from sediment roughness is the actual mechanism.

Acknowledgment

This work was supported by the U.S. Office of Naval Research, Code 321OA.

References

[1] N. P. Chotiros, "Biot model of sound propagation in water-saturated sand," *J. Acoust. Soc. Am.*, vol. 97, pp. 199–214, January 1995.

[2] J. L. Lopes, "Observations of anomalous acoustic penetration into sediment at shallow grazing angles," *J. Acoust. Soc. Am.*, vol. 99, pp. 2473–2474, April 1996.

[3] A. A. Maradudin, T. Michel, A. R. McGurn, and E. R. Mendez, "Enhanced backscattering of light from a random grating," *Annals of Physics*, vol. 203, pp. 255–307, November 1990.

[4] E. I. Thorsos, "The validity of the Kirchhoff approximation for rough surface scattering using a Gaussian roughness spectrum," *J. Acoust. Soc. Am.*, vol. 83, pp. 78–92, January 1988.

[5] J. E. Moe, "Near and far-field acoustic scattering through and from two dimensional fluid-fluid rough interfaces," Technical Report APL-UW TR 9606, Applied Physics Laboratory, University of Washington, October 1996.

[6] L. M. Brekhovskikh, *Waves in Layered Media*, San Diego, Academic Press, 1980.

[7] S. Stanic, K. B Briggs, P. Fleischer, R. I. Ray, and W. B. Sawyer, "Shallow-water high-frequency bottom scattering off Panama City, Florida," *J. Acoust. Soc. Am.*, vol. 83, pp. 2134–2144, June 1988.

[8] P. D. Mourad and D. R. Jackson, "High frequency sonar equation models for bottom backscatter and forward loss," in *Proceedings of OCEAN '89*, IEEE Press, vol. 4, pp. 1168–1175, 1989.